process would still require about 2.1 eV. This suggests an estimate for the internal energy of $[Mn_2(CO)_{10}]^+$ to be about 1.7 eV. This compares with the results of our RRKM calculations, which found an internal energy of about 1.7 eV.

The observed CID threshold energy for $[Mn_2(CO)_8]^+$ would be -0.3 eV based upon the above arguments. However, $[Mn_2(CO)_8]^+$ was not observed as an abundant CID or unimolecular dissociation fragment. This could be due to a concerted loss of two CO ligands from $[Mn_2(CO)_9]^+$. It could also be due to competing channels for the fragmentation of $[Mn_2(CO)_9]^+$. The following reaction is also expected due to the stability of $^{\bullet}Mn(CO)_5$, an 18-electron radical species:

$$[Mn_2(CO)_9]^+ \rightarrow [Mn(CO)_4]^+ + {}^{\bullet}Mn(CO)_5 \qquad (13)$$

In fact, the presence of these two channels, the loss of two CO ligands versus the loss of $^{\bullet}Mn(CO)_5$, is suggestive of the presence of two geometric isomers of $[Mn_2(CO)_9]^+$. An isomer with a bridging carbonyl between the Mn atoms could lose two pendant CO ligands more readily than cleaving the bridged Mn-Mn bond. On the other hand, an isomer without bridging carbonyls could lose $^{\bullet}Mn(CO)_5$ via a single bond cleavage.

Formation of $[Mn(CO)_4]^+$ can arise from at least two channels. The corrected CID threshold energy of 2.8 eV in Table III was obtained by assuming an internal energy of 1.7 eV added to the observed threshold energy. The loss of $^{\bullet}Mn(CO)_5$ in eq 13 corresponds to cleavage of the Mn-Mn bond. Assuming a threshold energy of 0.7 eV for $[Mn_2(CO)_9]^+$ gives an upper limit of 2.1 eV for $D[(CO)_4Mn^+-Mn(CO)_5]$. Similarly, the loss of a CO from $[Mn(CO)_5]^+$ gives rise to $[Mn(CO)_4]^+$. Assuming $D[(CO)_4Mn^+-CO] = 0.7$ eV gives an upper limit of 2.1 eV for $D[(CO)_5Mn^+-Mn(CO)_5]$. Because both estimated values are similar, it is impossible to guess which channel produces the $[Mn(CO)_4]^+$ fragment. However, the loss of additional CO ligands might be expected to strengthen the Mn-Mn bond. In fact, experiments on the CID of $[Mn_2(CO)_2]^+$ indicate that in this ion the appearance of the $[Mn(CO)_2]^+$ fragment has a threshold of about 2.1 eV.[33] This indicates either a much stronger Mn-Mn bond or the more than likely presence of bridging carbonyls. Thus, it is likely that $[Mn(CO)_x]^+$ ($x = 1-3$) arise from sequential losses of CO ligands and not from dissociations of dimetal ions.

Conclusions

The dissociation of gas-phase, long-lived metastable $[Mn_2(CO)_{10}]^+$ depends primarily on the temperature of the neutral molecules in the ion source before ionization. Thus, it appears the temperature of the neutral molecules alters or affects the potential surface for unimolecular dissociation of the ion. The rate constants for the metastable dissociations and their relative abundance reflect the amount of internal energy required for the fragmentation. The use of a tandem mass spectrometer permits the kinetic analysis of ions in a time regime (10-100 μs) where ions with relatively low (ca. 1 eV) internal energy can dissociate. The formation of the fragment ions appears to proceed via stepwise loss of the CO ligands. The individual Mn-CO bond dissociation energies tend to average about 0.7 eV, in good agreement with other techniques. Statistical rate conclusions based upon the unimolecular dissociation rate and an Mn-Mn bond dissociation energy of 0.95 eV estimate that the internal energy of the ions is about 1.7 eV, also in agreement with results for the CID threshold energy of $[Mn_2(CO)_7]^+$. Consideration of a corrected CID threshold energy for $[Mn(CO)_4]^+$ gives an upper limit to the Mn-Mn bond dissociation in $[Mn_2(CO)_9]^+$ and $[Mn_2(CO)_{10}]^+$ of 2.1 eV. It has been shown that a careful analysis of the low-energy energy-resolved CID of ions must be made to precisely determine bond dissociation energies from CID thresholds.[14] It appears from the results of this work that differences between thresholds can be obtained that correspond to individual bond dissociation energies for simple, sequential ligand losses. Differences in threshold energies, which are of a magnitude greater than expected, may correspond to different structural isomers, i.e., such as clusters containing bridging carbonyls.[33]

Acknowledgment. The Robert A. Welch Foundation is acknowledged for support of this work. The instrumentation was purchased with funds from the Texas Advanced Research Technology Program. We thank Prof. D. P. Ridge for helpful discussions.

(33) Yu, W.; Freas, R. B. Energy-Resolved Collision-Induced Dissociation of Dimanganese Carbonyl Cluster Fragment Ions in the Gas phase. Evidence for Multiple Bridging Carbonyls in Coordinatively Unsaturated Species. Manuscript in preparation.

Free Energy Dependence of the Intrinsic Rate of Electron Transfer in Diffusional Quenching of *trans*-Stilbene S_1 by Electron-Deficient Olefins

Stephen A. Angel and Kevin S. Peters*

Department of Chemistry and Biochemistry, University of Colorado, Boulder, Colorado 80309-0215
(Received: June 27, 1990; In Final Form: November 9, 1990)

The quenching of the first excited singlet states of *trans*-stilbene and 4,4'-dimethyl-*trans*-stilbene by acrylonitrile, fumaronitrile, and tetracyanoethylene has been examined by picosecond laser spectroscopy. The intrinsic rate constant of electron transfer is separated from the diffusion rate constant by applying the Collins and Kimball formalism for time-dependent rate constants. The intrinsic rates of electron transfer are correlated with the free energy changes for electron transfer, and it is found that the correlation does not follow the predictions of Marcus' adiabatic electron-transfer theory.

Introduction

The transfer of an electron between a molecular donor molecule and an acceptor is one of the most fundamental chemical reactions found in both chemistry and biochemistry.[1] As such, the electron-transfer reaction has been the subject of numerous theoretical studies. From the treatment of Marcus,[2] employing transition-state

SCHEME I

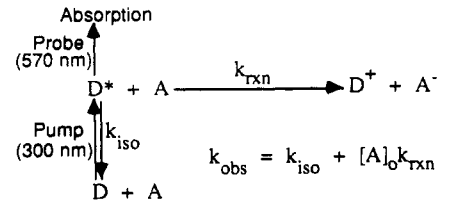

(1) Some examples are the following. Respiration and photosynthesis: Gray, H. B.; Malmstrom, B. G. *Biochemistry* **1989**, *28*, 7499. Silver halide sensitization: Gilman, P. G. *Pure Appl. Chem.* **1977**, *49*, 357. Photoinduced polymerization: Eaton, D. F. In *Advances in Photochemistry*; Volman, D. H., Gollniock, K., Hammond, G. S., Eds.; Wiley: New York, 1986; Vol. 13. *Organic and inorganic photochemistry*: Mattes, L. L.; Farid, S. In *Organic Photochemistry*; Padwa, A., Ed.; Marcel Dekker: New York, 1986; Vol. 6.

0022-3654/91/2095-3606$02.50/0

theory in conjunction with a continuum description for the nonequilibrium polarization of the medium, to the quantum-mechanical formalism of Levich,[3] each theory predicts a maximum rate for electron transfer when the reorganization energy, λ, matches the negative free energy change, $-\Delta G$, between reactant and product. For reaction energies more negative than the positive reorganization energy, the rate of electron transfer decreases with decreasing free energy change for the reaction, leading to the so-called "inverted region".

There have been numerous experimental investigations probing for the existence of the inverted region. By examining intramolecular electron transfer within a radical anion where the donor and acceptor moieties are separated by a steroid spacer, Miller and Closs[4] observed the predicted Marcus behavior for electron transfer. Farid and co-workers[5] found evidence for the existence of the inverted region in their studies of electron transfer within a radical-ion pair that decays to produce a pair of neutral molecules. Among the more interesting and intriguing studies that did not display kinetic behavior consistent with the inverted region are the nanosecond fluorescence quenching experiments of Rehm and Weller,[6] where they examined the energy dependence of the rate of quenching of excited singlet states by electron transfer to produce radical-ion pairs; the rate of quenching approaches a maximum value of approximately 2×10^{10} M^{-1} s^{-1} and remains constant with increasing energy changes for the electron transfer.

One possible criticism of the Rehm and Weller experiments is that for highly exoergic electron-transfer reactions the intrinsic rate of electron transfer is greater than the rate of diffusion, so that the rate of quenching of the excited singlet state becomes limited by diffusion. In other words, the quenching rate of 2×10^{10} M^{-1} s^{-1} reflects a reaction limited by diffusion and not the intrinsic rate of electron transfer.

Recently, we reported[7] a picosecond study of the quenching of the first excited singlet state of *trans*-stilbene by fumaronitrile that proceeds through electron transfer. From the formalism developed by Collins and Kimball[8] for time-dependent rate coefficients to analyze the quenching data, the intrinsic rate of electron transfer and the rate of diffusion can be separated. In this paper, we extend this study to include electron transfer from the donors *trans*-stilbene and 4,4'-dimethyl-*trans*-stilbene to the acceptors acrylonitrile, fumaronitrile, and tetracyanoethylene and discuss the relationship between the rates of electron transfer and the corresponding energy changes.

Experimental Section

Picosecond Absorption Spectrometer. The picosecond laser system has been described previously.[7b,9] Briefly, a mode-locked Nd:YAG laser (Spectra-Physics 2000) synchronously pumps a dye laser (Spectra-Physics 375B) to produce a 1-ps pulse at 600 nm. The output is passed through a three-stage pulse dye amplifier pumped by a Q-switched Nd:YAG laser (Quanta Ray DCR-2), which outputs pulses at 10 Hz, 1 ps, 1.1 mJ, and 600 nm. This light is frequency-doubled to 300 nm (5% efficiency) to form the excitation pulse, and the residual 600-nm light is then focused into a 5-cm cell of H_2O/D_2O to produce continuum light from 450 to 750 nm for the probe pulse. The probe pulse is then split into I and I_0 pulses, which are detected by two photodiodes (EG&G SGD Series) interfaced to two boxcar integrators (Stanford Research Systems) whose output is passed to a laboratory computer (PDP 11/23). At each time delay, 200 laser shots with the excitation pulse and without the excitation pulse are averaged.

Samples. The three electron acceptors employed in this study were acrylonitrile (AN), fumaronitrile (FN), and tetracyanoethylene (TCE), which were obtained from Aldrich. Tetracyanoethylene was sublimed twice. Fumaronitrile was dissolved in dichloromethane, the solution filtered, and the solvent rotary-evaporated; the sample was then sublimed. The electron donors were *trans*-stilbene (TS) and 4,4'-dimethyl-*trans*-stilbene (DMES). *trans*-Stilbene was obtained from Aldrich and recrystallized from ethanol. 4,4'-Dimethyl-*trans*-stilbene was synthesized as previously described.

Diffusion Coefficients. Diffusion coefficients were determined by using the chronocoulometric mode on a BAS 100 electrochemical analyzer, as previously described.[7] The values for TS, DMES, FN, and TCE are given in Table I.

TABLE I: Diffusion Coefficients for Solutes, Measured in Acetonitrile

solute	electrochemical diffusion coeff, $Å^2$ ps^{-1}	estd[a]
TS	0.16 ± 0.02	0.19
DMES	0.12 ± 0.01	0.14
FN	0.12 ± 0.01	0.14
TCE	0.081 ± 0.001	0.10

[a] Values are 20% larger than experimentally determined diffusion coefficients of solutes in solution of acetonitrile with 0.1 M tetrabutylammonium fluoroborate: these values are used to calculate D in eqs 3–7.

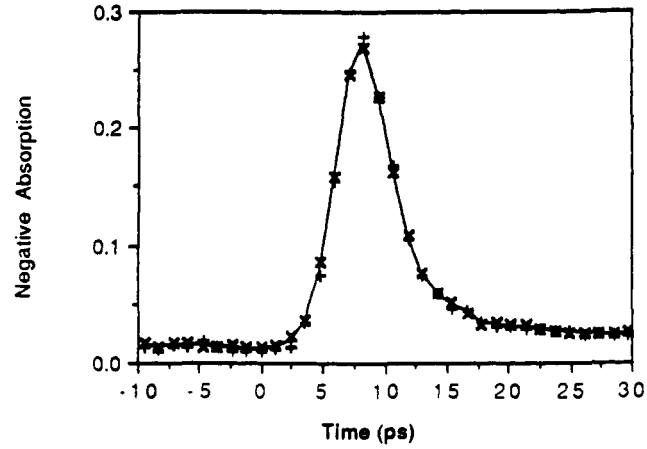

Figure 1. Pump/probe bleaching of the ground state of crystal violet in methanol at negative and long times. The line is an average of the experimental data: +, first experimental data set; ×, second experimental data set.

Data Analysis

Instrument Response. The convolution of the instrument response function $I(t)$ with the chemical kinetics signal $F(t)$ produces the observed absorption change $A(t)$ according to[10]

$$A(t) = \int_0^t I(t - x)\, F(x)\, dx \qquad (1)$$

Initially, the function $I(t)$ is obtained, given a predetermined $F(t)$. In the absence of electron acceptors, the excited singlet states of TS and DMES relax to the ground states through an isomerization channel.[11,12] Long-time kinetics, $20 < t < 300$ ps, of the decay

(2) Marcus, R. A. *J. Chem. Phys.* **1956**, *24*, 966; **1957**, *26*, 867, 872. Marcus, R. A. *Can. J. Chem.* **1959**, *37*, 155. Marcus, R. A.; Sutin, N. *Biochim. Biophys. Acta* **1985**, *811*, 265.

(3) Levich, V. G. In *Physical Chemistry: An Advaned Treatise*; Erying, H., Henderson, D., Jost, W., Eds.; Academic Press: New York, 1970; Vol. 9B. See also: Ulstrup, J.; Jortner, J. *J. Chem. Phys.* **1975**, *63*, 4358. Kestner, N.; Logan, J.; Jortner, J. *J. Phys. Chem.* **1974**, *78*, 2148.

(4) Miller, J. R.; Calcaterra, L. T.; Closs, G. L. *J. Am. Chem. Soc.* **1984**, *106*, 3047. Closs, G. L.; Calcaterra, L. T.; Green, N. J.; Penfield, K. W.; Miller, J. R. *J. Phys. Chem.* **1986**, *90*, 3673. Closs, G. L.; Miller, J. R. *Science* **1988**, *240*, 440.

(5) Gould, I. R.; Ege, D.; Mattes, S. L.; Farid, S. *J. Am. Chem. Soc.* **1987**, *109*, 3794; **1988**, *110*, 1991. Gould, I. R.; Moser, J. E.; Ege, D.; Moody, R.; Armitage, B.; Farid, S. *J. Imaging Sci.* **1989**, *33*, 44.

(6) Rehm, D.; Weller, A. *Isr. J. Chem.* **1970**, *8*, 259.

(7) (a) Angel, S. A.; Peters, K. S. *J. Phys. Chem.* **1989**, *93*, 713. (b) Angel, S. A. Ph.D. Thesis, University of Colorado, Boulder, CO, 1989.

(8) Collins, F. C.; Kimball, G. *J. Colloid Sci.* **1949**, *4*, 425.

(9) Koch, T. L.; Chiu, L. C.; Yariv, A. *Opt. Commun.* **1982**, *40*, 364.

(10) Demas, J. N. *Excited State Lifetime Measurements*; Academic: New York, 1983.

(11) Rothenberger, G.; Negus, D. K.; Hochstrasser, R. M. *J. Chem. Phys.* **1983**, *79*, 5360.

TABLE II: Summary of Calculated and Experimentally Determined Parameters for Electron-Transfer Reactions in Acetonitrile

reactants[a]	products[a]	ΔG,[b] kcal/mol	k_{et},[c] M^{-1} s^{-1}	$10^{-10}k_d$,[c] M^{-1} s^{-1}	R,[c] Å
TS*/AN	TS^+/AN^-	+7.1	$(2.6 \pm 0.1) \times 10^9$	...	
DMES*/AN	$DMES^+/AN^-$	+4.6	$(5.6 \pm 0.1) \times 10^9$	...	
TS*/FN	TS^+/FN^-	−17.5	$(3.0 \pm 1.0) \times 10^{11}$	2.2	8.7
DMES*/FN	$DMES^+/AN^-$	−20.1	$(4.0 \pm 0.6) \times 10^{11}$	2.2	10.5
TS*/TCE	TS^+/TCE^-	−52.8	$(4.5 \pm 1.2) \times 10^{11}$	2.3	10.5
DMES/TCE	$DMES^+/TCE^-$	−55.3	$(4.0 \pm 1.2) \times 10^{11}$	2.0	11.0
TS*/TCE	TS^{+*}/TCE^-	−14.7			
TS*/TCE	TS^+/TCE^{-*}	+10.6			
DMES/TCE	$DMES^{+*}/TCE^-$	−16.1			
DMES/TCE	$DMES^+/TCE^{-*}$	+8.1			

[a] The symbols *, +, and − represent excited electronic states and positive and negative formal charges, respectively. [b] The change in the free energy of the reaction is calculated from eq 8. [c] Both k_{et} and R represent best fits to the data; k_d is given by eq 4.

of these states establishes an $F(t)$ independent of $I(t)$. The isomerization kinetics at early time, $0 \le t < 100$ ps, is then fit to eq 1, with $F(t)$ known, to generate $I(t)$.

Interestingly, the function $I(t)$ can be observed from the bleaching of the ground state of crystal violet[13] (Figure 1). The pulse is not symmetrical. The "rise" is fit to a Gaussian, and the "fall" is fit to a Lorentzian. In addition, there is a persistent baseline absorption, BA, due to the detection of amplified spontaneous emission, ASE (generated at the pulse dye amplifier). $I(t)$ is therefore composed of two functions, $G(t)$ and $L(t)$, and the observed absorption for chemical kinetics is given by

$$A(t) = \int_0^{t_m} G(t-x)\,F(x)\,dx + \int_{t_{m'}}^{t} L(t-x)\,F(x)\,dx + BA \qquad (2)$$

Here, $G(t) = N_1 \exp[-(t-c)^2/2\sigma^2]$ is the Gaussian rise, and $L(t) = N_2[(1/\tau)^2 + (t-\omega)^2]^{-1}$ represents the Lorentzian decay of the instrument response. BA is a constant. The best fit for the instrument response function for the crystal violet bleaching experiment ($F(x) = 1$) is shown in Figure 2.

After the instrument response function is determined, the transient absorption data are analyzed according to Scheme I. In the presence of an electron acceptor, A, the excited singlet state, D*, either is quenched or undergoes isomerization to the ground state with respective rate constants k_{rxn} and k_{iso}. The functional form of k_{rxn} is the focal interest: from it the electron-transfer rate constant, k_{et}, is obtained.

Kinetic Models. For the electron-transfer reactions that quench the excited singlet state of *trans*-stilbene, two kinetic processes (with associated rate constants) will be of interest: electron transfer (k_{et}) and diffusion (k_d). If the electron-transfer rate constant $k_{et} \ll k_d$, then the rate of quenching will depend predominantly upon k_{et}. Conversely, if $k_{et} \gg k_d$, diffusion is the rate-limiting step. It follows that when $k_{et} \approx k_d$, the observed rate will depend on both k_{et} and k_d.

The kinetic theory for diffusion-controlled reactions ($k_{et} \gg k_d$) was originally developed by Smoluchowski.[14] Solving Fick's law of diffusion with the boundary condition that the concentration of reactants is zero at the surface of a sphere of radius R, the reaction distance, yields

$$k_S(t) = k_d[1 + R(\pi Dt)^{-1/2}] \qquad (3)$$

where

$$k_d = 4\pi R N_A (D_D + D_A) \qquad (4)$$

The quantity $D_D + D_A$ is the sum of the diffusion coefficients for the donor and acceptor molecules, N_A is Avogadro's number, and R is the sum of the spherical reactants' radii.

The theory for solution-phase kinetics when $k_{et} \ge k_d$ was developed by Collins and Kimball.[8] If a small barrier exists at radius

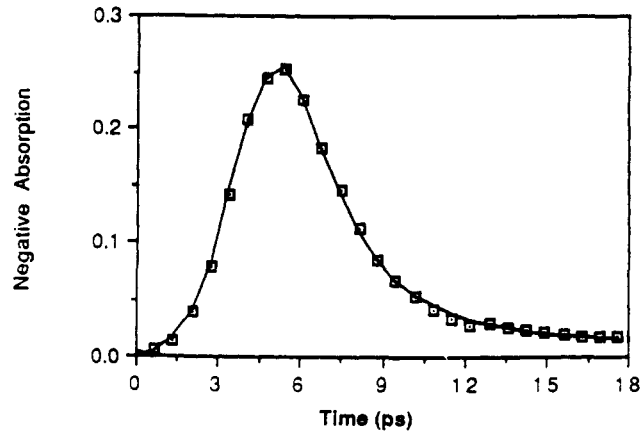

Figure 2. Ground-state bleaching of crystal violet, fit to the instrument response function, eq 2, with $F(t) = 1$. The following parameters are defined in the text: $\sigma = 2.01$ ps, $c = 5.06$ ps, $\tau^{-1} = 1.35$ ps, $\omega = 4.07$ ps, $t_m = 5.4$ ps (9th data point), $t_{m'} = 6.1$ ps (10th data point), BA = 0.003. The magnitude of absorption at negative times is reduced to zero. The squares represent data; the solid line is the calculated fit.

R, the probability of reactants going to products is "κ", not unity, and the concentration, c, of reactants at $r = R$ need not be zero. The solution to Fick's second law of diffusion with the boundary condition $c(R) = (D/\kappa)(\delta c/\delta r)_R$ yields

$$K_{CK}(t) = [k_{et}^{-1} + k_d^{-1}]^{-1}[1 + (k_{et}/k_d)\exp(y^2)\,\mathrm{erfc}\,(y)] \qquad (5)$$

where

$$\mathrm{erfc}\,(y) = (2\pi)^{-1/2}\int_Y^\infty \exp(-u^2)\,du \qquad (6)$$

and

$$y = [(Dt)^{1/2}/R][1 + (k_{et}/k_d)] \qquad (7)$$

Parenthetically, the limits of eq 5 are well-behaved: for $k_{et} \gg k_d$, $k_{CK}(t) = k_S(t)$; for $k_{et} \ll k_d$, $k_{CK}(\text{time independent}) = (k_{et}^{-1} + k_d^{-1})^{-1}$; and, as $t \to 0$, $k_{CK} \to k_{et}$.

Energetics. In the ensuing study of electron-transfer reactions, we will examine the transfer of electrons from the excited singlet state of stilbenes to electron-deficient olefins. The free energy change for this reaction has been approximated[6,15] by the difference between the reactant and product equilibrium free energies given by eq 8, in which E_D^{ox} is the oxidation potential of the ground-state

$$\Delta G_{et} = E_D^{ox} - E_A^{red} - E_D^S - (e_0^2/\epsilon a) \qquad (8)$$

stilbene, E_A^{red} is the reduction potential of the electron-deficient olefin, E_D^S is the energy of the excited singlet state of stilbene, and $(e_0^2/\epsilon a)$ is the Coulombic stabilization of the product radical-ion pair. From the bulk dielectric constant of acetonitrile, the stabilization energy is calculated to be small,[15] approximately 0.1 eV, for the contact radical-ion pair and is omitted in further determination of ΔG_{et}. Table II lists the free energy changes for electron transfer for the stilbene/olefin pairs that were investigated.

(12) Courtney, S. H.; Fleming, G. R. *J. Chem. Phys.* **1985**, *83*, 215.
(13) Shank, C. V.; Ippen, E. P.; Teschke, O. *Chem. Phys. Lett.* **1977**, *45*, 291.
(14) Smoluchowski, M. *Z. Phys. Chem., Stoechiom. Verwandtschaftsl.* **1917**, *92*.
(15) Lewis, F. D. *Adv. Photochem.* **1986**, *13*, 165.

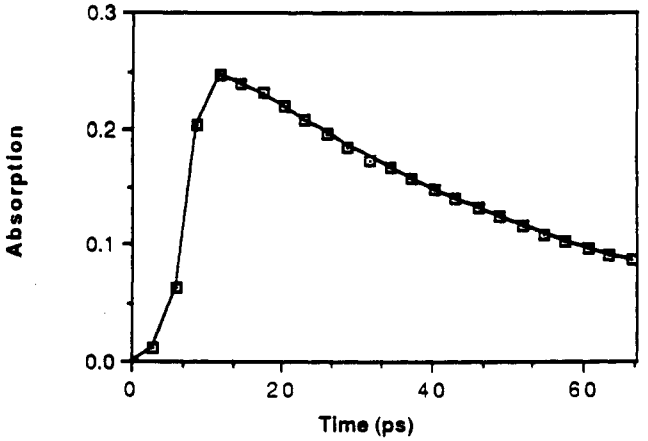

Figure 3. Absorption of the *trans*-stilbene excited singlet state (TS*) as a function of time. The fit is a convolution of a single-exponential decay with the instrument response function, eq 2. The lifetime was predetermined and set at 43.5 ps. The squares represent data; the solid line is the calculated fit.

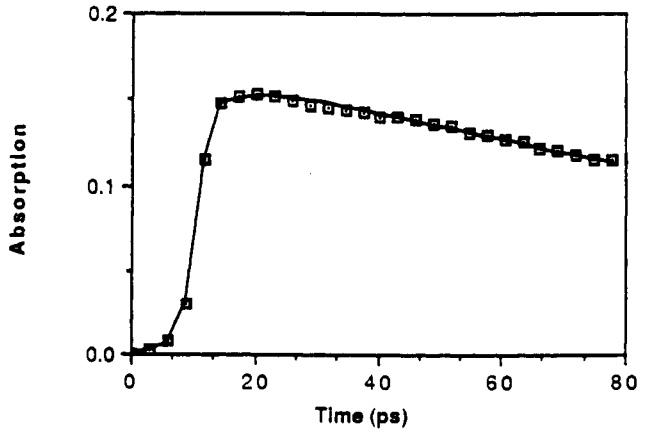

Figure 4. Absorption of the 4,4'-dimethyl-*trans*-stilbene excited singlet state (DMES*) as a function of time. The fit is a convolution of a single-exponential decay with the instrument response function, eq 2. The predetermined lifetime used in the fit is 136 ps. The squares represent data; the solid line is the calculated fit.

The values for the oxidation and reduction potentials as well as the energies for the excited singlet states were taken from the literature.[15-17]

Results

Excited-State Dynamics of TS and DMES. The dynamics of the decays of the first excited singlet states of *trans*-stilbene (TS*) and 4,4'-dimethyl-*trans*-stilbene (DMES*), following 300-nm excitation to TS and DMES, are monitored at 570 nm near the $S_n \leftarrow S_1$ absorption maximum[18] (Figures 3 and 4). Assuming the isomerization decay[11,12] of S_1 can be characterized by an exponential relaxation, the lifetime for TS* is 42.5 ± 2.5 ps and the lifetime of DMES* is 136 ± 3 ps, both in acetonitrile at 21 °C. The best fits to the experimental data employed eq 2; these are also shown in Figures 3 and 4. As mentioned, this fitting procedure was used to establish an instrument response function for a given series of experiments that was subsequently held constant for the kinetic analysis of the series of electron-transfer reactions.

In a prior investigation[7] of the quenching of TS* by fumaronitrile, the lifetime of TS* was reported as 48 ± 3 ps. We attribute this difference to the choice of the analytical form of the instrument response function and our failure to account for a baseline absorption due to the continual absorption of ASE. Neglecting a 1.5% baseline absorption results in an 11% increase in the measured lifetime.

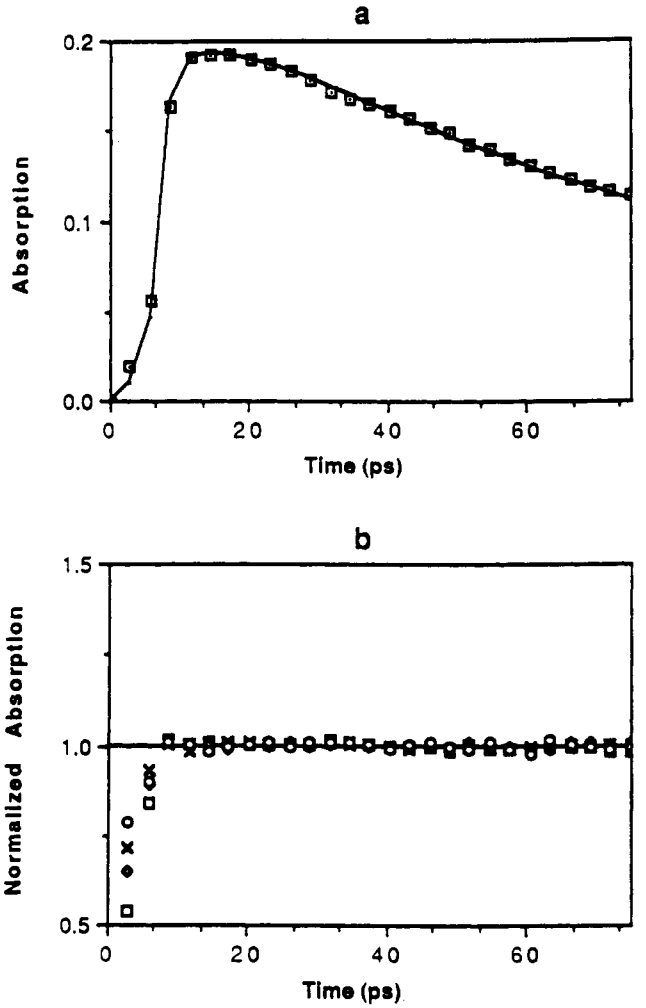

Figure 5. Kinetics of the DMES* reaction with AN in acetonitrile. Data are fit to a single-exponential decay. The two fitting parameters are an absorption coefficient and a pseudo-first-order rate constant. (a) Absorption of DMES* in the presence of 0.760 M AN: squares, data; solid line, calculated fit. (b) Normalized fits at varying concentrations (0.46 M, 0.76 M, 1.5 M, and 2.3 M) of AN.

Quenching of TS and DMES* by AN.* In the presence of AN, the population of excited stilbenes may be depleted by isomerization or electron transfer, according to Scheme I. The simplest analytical form for the kinetics of the observed quenching is given by eq 9, where k_{iso} is the unimolecular decay constant of the excited

$$k_{obs} = k_{iso} + k_{et}[AN]_0 \quad (9)$$

singlet state, determined in the prior experiment, in the absence of the quencher AN. The absorption of DMES* in the presence of 0.76 M AN is shown in Figure 5a. The best fit is obtained by using eq 2 with $I(t)$ and k_{iso} predetermined (Figure 4); $F(t)$ is a single-exponential decay with an observed rate constant, k_{obs}, given by eq 9. k_{obs} is linear versus all concentrations of AN when k_{iso} is constant. Normalized fits to the absorption of DMES* in the presence of varying concentrations of AN are presented in Figure 5b. The errors in the fits at times <8 ps, observed in Figure 5b, are attributed to a poor fit to the instrument response parameters, which are held constant: either the instrument response is not well-defined by the previous fits, or the temporal pump and probe pulse shapes vary over the time of data acquisition.

To obtain an accurate value of k_{et} in eq 9 for the quenching of TS* and DMES*, the concentration of AN in solution with TS was varied from 0.30 to 4.6 M and the concentration of AN in solution with DMES was varied from 0.46 to 2.3 M. The observed pseudo-first-order rate constant, k_{obs}, when correlated with the concentration of AN, yields the second-order rate constant for electron transfer, k_{et}. The rate constant for the quenching of

(16) Freilich, S. C.; Ph.D. Thesis, Harvard University, Cambridge, MA, 1983.
(17) Adams, B. K.; Cherry, W. R. *J. Am. Chem. Soc.* **1981**, *103*, 6904.
(18) Hochstrrasser, R. M. *Pure Appl. Chem.* **1980**, *52*, 2683.

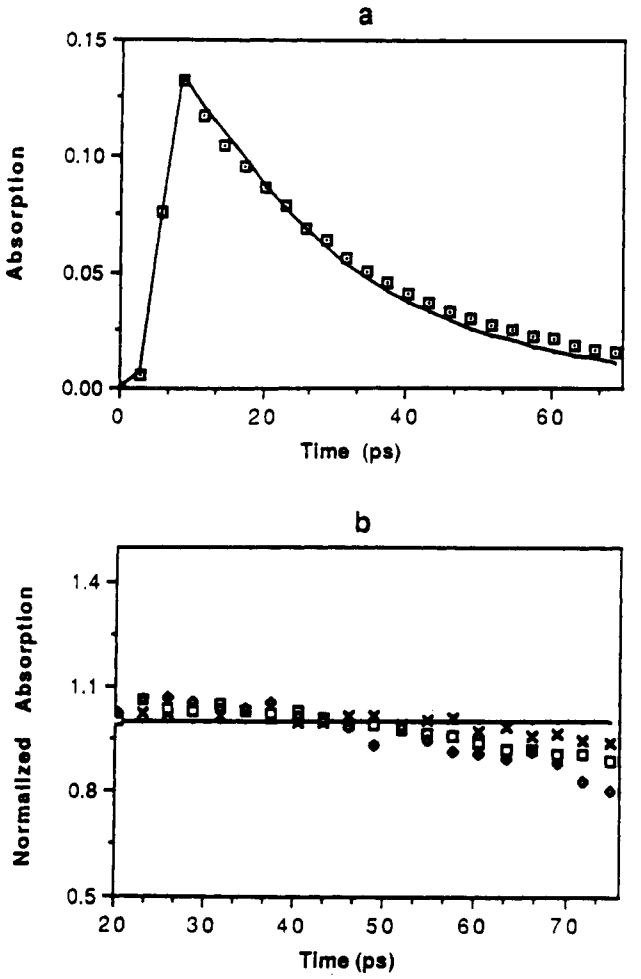

Figure 6. (a) Instrument response function is convolution with a single-exponential decay, fit to the absorption data of TS* in solution with 0.33 M FN: squares, data; solid line, calculated fit. (b) Normalized exponential decay fits to the absorption of DMES* in solutions varying in FN concentration: ×, 0.31 M; □, 0.46 M; ◇, 0.58 M.

TS* by AN to produce the radical-ion pair composed of the radical cation to *trans*-stilbene (TS^+) and the radical anion of acyronitrile (AN^-) is $(2.6 \pm 0.1) \times 10^9$ M^{-1} s^{-1}. The rate constant for electron transfer between DMES* and AN to form the radical cation of 4,4′-dimethyl-*trans*-stilbene ($DMES^+$) and the radical anion AN^- is $(5.6 \pm 0.1) \times 10^9$ M^{-1} s^{-1}.

The free energy changes for the quenching of TS* and DMES* by AN fall within the Marcus normal region[19,20] for electron transfer, as both processes are slightly endoergic: ΔG_{et} for TS*/AN is +7.1 kcal/mol and for DMES*/AN is 4.6 kcal/mol. As the free energy for electron transfer decreases, the rate constant increases from 2.6×10^9 to 5.6×10^9 M^{-1} s^{-1}, characteristic of the normal region for electron transfer. It is noted that these rate constants for electron transfer are less than those for diffusion-controlled processes.

Quenching of TS and DMES* by FN.* The decay of TS* in the presence of 0.33 M FN in acetonitrile is shown in Figure 6a. Normalized absorption for the decay of DMES* with various concentrations of FN is shown in Figure 6b. Whereas the dynamics of the decays of TS* and DMES* in the presence of AN were well characterized by the convolution of a single time-independent exponential decay with the instrument response function given in eq 2, the observed decay of these two electron donors in the presence of FN is poorly described by a single time-independent exponential decay (Figure 6). In particular, the decays are faster at earlier times and slower at longer times than predicted by the time-independent fit.

(19) (a) Marcus, R. A. *Discuss. Faraday Soc.* **1960**, *No. 29*, 21. (b) Siders, P.; Marcus, R. A. *J. Am. Chem. Soc.* **1981**, *103*, 748.
(20) Marcus, R. A.; Siders, P. *J. Phys. Chem.* **1982**, *86*, 622.

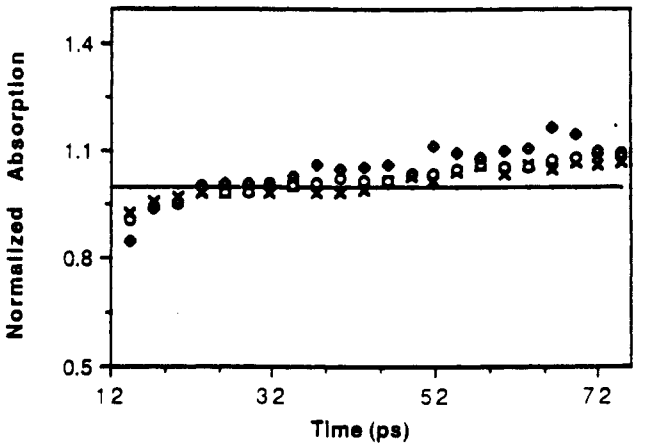

Figure 7. Normalized fit for data presented in Figure 6b with the rate constant given in Scheme I, k_{rxn}, replaced by k_S, eq 3: ×, 0.31 M, FN; ○, 0.46 M FN; ◇, 0.58 M FN.

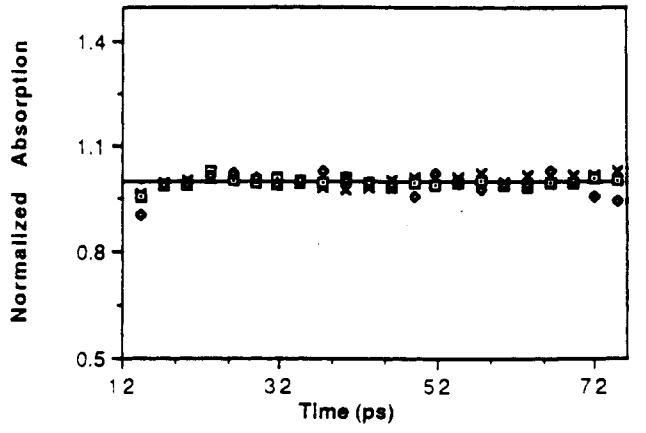

Figure 8. Normalized fit for data presented in Figure 6b with the rate constant given in Scheme I, k_{rxn}, replaced by k_{CK}, eq 5: ×, 0.31 M FN; □, 0.46 M FN; ◇, 0.58 M FN.

Since the dynamics of the decays of TS* and DMES* in the presence of FN were poorly characterized by a single time-independent exponential decay, an attempt was made to fit the data to the Smoluchowski equation,[14] eq 3, where the observed rate constant is time dependent. In the Smolchowski equation, the reaction distance R is allowed to vary. In addition, the diffusion coefficients D are varied from the values determined electrochemically to values that are 20% larger. Electrochemical diffusion coefficients are determined with the aid of 0.1 M electrolyte. Recent experiments[21] show that a 0.1 M concentration of tetrabutylammonium fluoborate (the electrolyte) in tetrahydrofuran may slow the diffusion of the analyte by approximately 20%. Conversely, there is no evidence of diffusive rate dependence on analyte concentration. Increasing the diffusion coefficient by 20%, therefore, is a rough approximation to the diffusive rate of the reacting solutes during the electron-transfer experiments.

The best fit of the Smoluchowski equation to the DMES*/FN data is shown in Figure 7. The fit for the data is a convolution of the instrument response function, eq 2, with a single-exponential decay whose rate constant is the sum of the first-order isomerization rate constant, k_{iso}, and the pseudo-first-order electron-transfer rate constant, $k_S(t)$, given by eq 3.

$$k_{obs}(t) = k_{iso} + k_S(t)\ [FN] \qquad (10)$$

The trend in the fit is opposite to that presented in Figure 6. Initially, the fit decays faster than the data, and at later times the fit decays slower than the data.

Analyzing the same data within the Collins and Kimball[8] framework produces the fits shown in Figure 8. As before, the fits are generated by a convolution of the instrument response

(21) T. Rutton and S. Strickler, University of Colorado, Boulder, CO, private communication, 1989.

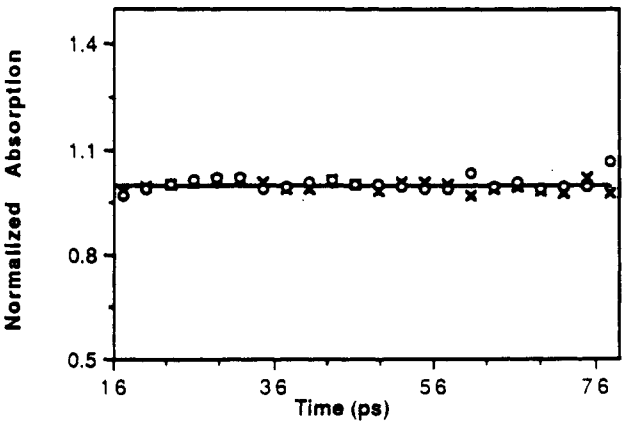

Figure 9. Normalized fits to the absorption of DMES* in AN with varying concentrations of TCE: ×, 0.30 M; O, 0.41 M. The kinetics of Scheme I are assumed with k_{rxn} replaced by k_{CK}, eq 5.

function with a single-exponential decay. The rate constant for the exponential decay is the sum of the isomerization rate constant and the pseudo-first-order constant given in eq 5. The fitting procedure involves assuming a value for R (Table II) and allowing the electron-transfer rate, k_{et}, to vary. R is then varied to achieve a best fit. Again, D is set at a value that is 20% larger than the electrochemical value. The best fit to the data for DMES*/FN for three different concentrations of FN is shown in Figure 8 for a given set of R, D, and k_{et}. The electron-transfer rate constant, k_{et}, determined in the best fit to the experimental data depends on the values for the radius R and the diffusion coefficient D. The effect of increasing D by 20% decreases k_{et} by a maximum of 40%. Increasing R by 20% decreases k_{et} by approximately 10%. The best fits applying the Collins and Kimball formalism to the experimental data for TS*/FN and DMES*/FN are given in Table II.

The free energy changes for the electron transfer between TS*/FN and DMES*/FN are −17.5 and −20.1 kcal/mol. The corresponding rate constants are k_{et}(TS*/FN) = (3.0 ± 1.0) × 10^{11} M^{-1} s^{-1} and k_{et}(DMES*/FN) = (4.0 ± 0.6) × 10^{11} M^{-1} s^{-1}. The dynamics of electron transfer is 1 order of magnitude greater than that of a diffusion-controlled process.

Quenching of TS and DMES* by TCE.* The kinetics for the quenching of TS* and DMES* by TCE in acetonitrile were examined for concentrations ranging from 0.1 to 0.41 M. Acceptable fits to the experimental data were only observed for a time-dependent rate constant described by the Collins and Kimball formalism (Figure 9). By use of the same procedure utilized in the analysis of the kinetic data for TS*/FN and DMES*/FN, the rate constants for electron transfer were obtained and are listed in Table II. The optimum values of rate constants for electron transfer are k_{et}(TS*/TCE) = (4.5 ± 1.2) × 10^{11} M^{-1} s^{-1} and k_{et}(DMES*/TCE) = (4.0 ± 0.7) × 10^{11} M^{-1} s^{-1}. The free energy changes for electron transfer between TS*/TCE and DMES*/TCE are highly exoergic, −52.8 and −55.3 kcal/mol, respectively.

Discussion

The most intriguing aspect of this series of experiments is the relationship between the rate of electron transfer and the corresponding free energy change for the reaction (Table II). When the reaction is endoergic, + 7.1 kcal/mol for TS*/AN, the rate of electron transfer is less than that for diffusion-controlled process, k_{et}(TS*/AN) = 2.6 × 10^9 M^{-1} s^{-1}. When the reaction becomes exoergic, −17.5 kcal/mol for TS*/FN, the rate constant increases to k_{et}(TS*/FN) = 3.0 × 10^{11} M^{-1} s^{-1}. Surprisingly, when the reaction becomes highly exoergic, −52.8 kcal/mol for TS*/TCE, the rate of electron transfer does not decrease as predicted by adiabatic Marcus electron-transfer theory[20,22] but rather remains constant within the error of the experiment, k_{et}(TS*/TCE) = 4.5 × 10^{11} M^{-1} s^{-1}. In essence, the experimental data of Table II can not be fit to an adiabatic expression for electron transfer for any values of v and λ in eq 11.

$$k_{et} = v \exp[-(\lambda + \Delta G)^2/4\lambda k_b T] \quad (11)$$

The reaction free energy changes, ΔG's calculated from eq 8 and listed in Table II, assume that the local, microscopic dielectric constant of the medium surrounding the product ion pairs approximates the bulk dielectric constant of the solvent. Although the magnitude of the deviation varies, the local dielectric constant is predictably less than the bulk value. Relative to the case governed by eq 8, this effect would lower the free energy of products formed within a solvent sphere of radius "a". This may explain why the electron-transfer rates between TS/AN and DMES/AN are at least 3 orders of magnitude faster than those calculated from eq 11, given reasonable values of v and λ and the ΔG's of Table II.

In the analysis of the kinetic data for the quenching experiments for TS*/FN, TS*/TCE, DMES*/FN, and DMES*/TCE, the rates of electron transfer were obtained from the Collins and Kimball formalism. This formalism assumes that there is an activated event whose rate, k_{act}, is greater than or equal to the rate of diffusion, k_d, and that as $t \rightarrow 0$, the observed rate of the reaction approaches k_{act}. In our modeling of the kinetics for the quenching of TS* and DMES*, we have assumed that as $t \rightarrow 0$, the rate of quenching is governed by electron transfer so that k_{et} is equated with k_{act}. If there is some other process that is limiting the quenching at early times, such as rotational diffusion of the reactants, then k_{act} is a measure not of the rate of electron transfer but rather of some other process. In this instance, the rate for quenching at early times, k_{act}, are lower bounds to the true rate of electron transfer, k_{et}. Even if only lower bounds for the rates of electron transfer are being determined, the relationship between the free energy for electron transfer and the corresponding rate constant clearly are not following the behavior predicted by Marcus' theory for adiabatic electron transfer. For reasonable values of the reorganization energy, λ = 1 eV, the rate constant for electron transfer for TS*/TCE is expected to be approximately 10^9 M^{-1} s^{-1} if the quenching of TS*/TCE is being governed by adiabatic electron transfer.

The contrasting behavior of the present experimental results and the Marcus theoretical predictions[20,22] given by eq 11 can be subject to numerous interpretations.

The simplest explanation for the plateau of rate constants noted by Rehm and Weller, RW, and subsequently noted here, considers the free energy of the product states initially created.[19b,23] Table II lists the free energy changes for TS*/TCE and DMES*/TCE electron-transfer reactions for which products in excited electronic states were formed. While the parabolic trend of eq 11 is not supported, the existence of an inverted region favors the initial creation of TS^+ and $DMES^+$ in excited electronic states. The contribution of these product states to the observed rate may be experimentally determined by comparing the absorption decay kinetics of TS* and DMES* (570 nm) with the rates of increase of TS^+ (470 nm) and $DMES^+$ (450 nm), respectively.

Early work[24] of Kakitani and Mataga explained the data of RW in terms of differential solvation. If a dielectric-continuum model of the solvent is not assumed, as it is in eq 11, the force constants that fashion the parabolic free energy potential surfaces in the solvent coordinate will not be the same for molecules and ions. Accordingly, in the polar solvent acetonitrile, there may be a lack of an inverted region because the charged product ions are more tightly solvated than the neutral reactant molecules. Their conclusions are subject to valid disagreement,[25,26] and their more recent equations[27] do not correlate well with the results of Table II.

(22) Marcus R. A. *Annu. Rev. Phys. Chem.* **1964**, *15*, 155; *J. Chem. Phys.* **1965**, *43*, 679.

(23) Beitz, J. V.; Miller, J. R. *J. Chem. Phys.* **1979**, *71*, 4579.

(24) Kakitani, T.; Mataga, N. *Chem. Phys.* **1985**, *93*, 381; *J. Phys. Chem.* **1985**, *89*, 4752.

(25) Carter, E. A.; Hynes, J. T. *J. Phys. Chem.* **1989**, *93*, 2184.

(26) Tachiya, M. *Chem. Phys. Lett.* **1989**, *159*, 505.

(27) Yoshimori, A.; Kakitani, T.; Yoshitaka, E.; Mataga, N. *J. Phys. Chem.* **1989**, *93*, 8316.

A model proposed by Efrima and Bixon[28] and others[29,30] amends eq 11 by considering the Franck–Condon factors for vibrational transitions. This theory leads to the prediction that excited vibrational states of the ground electronic product state are formed for reactions where $\Delta G + \lambda < 0$. In terms of eq 11, energy from available product vibrational modes, E_v, is added to the electronic-ground-state free energy change of the reaction until $\Delta G + E_v + \lambda = 0$. The significance of these quantum effects could be experimentally tested by comparing the absorption decays of excited singlet states with the growth of their respective cations' absorptions.

In the formulations of eq 5, used to obtain the electron-transfer rate constants, and eq 11, relating the rate of electron transfer to free energy and solvent reorganization changes, a distribution of reactants and products is neglected. Both equations assume reactants at an encounter distance, R. The best fit R values listed for TS/FN and DMES/FN in Table II correspond to center-to-center edge-on contact van der Waals radii between these two sets of reactants. If the larger R values listed for reactant sets TS/TCE and DMES/TCE are valid, eqs 5 and 11 would not be explicitly applicable. A more general representation of electron-transfer reactions includes radial[20,31] and geometrical[32] distributions of reactants and products. For a reaction at $r = R$, involving neutral reactants, large relative to the solvent, the bimolecular rate constant given in eq 11 follows from eq 12.

$$k_{et} = \kappa \int_R^\infty (\exp[-\alpha(r - R)])(\exp[-\Delta G^*(r)/kT])r^2\, dr \qquad (12)$$

Consistent with eq 11, $\Delta G^*(r) = [(\lambda(r) + \Delta G)^2/4\lambda]$, and κ is approximately[31] 10^{13} M^{-1} s^{-1}. The contributions to the observed k_{et} from reactions at $r > R$ will then obviously depend on the values of α, about 2 $Å^{-1}$ [33], and ΔG.

The radial and, depending on the shape of the reactants, geometrical dependences of the reorganization energy are due to the solvent.[31] In the normal region ($\lambda + \Delta G > 0$), the maximum rate constant is produced when solvent molecules are perturbed minimally during the reaction. This would correspond to the reactants forming contact ion pairs[7,34] at $r = R$, where the local change in dielectric constant would not be as great as if two separate ions were independently solvated, as in the case of solvent-separated ion pairs. When this argument is extended to the inverted region ($\lambda + \Delta G < 0$), contributions to the observed rate from reactants at $r > R$ become important as $\lambda(r) + \Delta G \rightarrow 0$. Classically, the preference for long-range electron transfer in solution may be influenced therefore by values of ΔG, $d\lambda(r)/dr$, and the ratio k_d/k_{et}, in addition to the effective solvent dielectric constant mentioned above. A study of the radial distribution of product states initially created in the electron-transfer reactions as a function of free energy change, solvent polarity, and viscosity is therefore of interest. In a previous communication,[7a] we reported the predominant formation of contact ion pairs in the reaction of TS and FN in acetonitrile. We have not yet employed this technique to study the systems TS/TCE and DMES/TCE in acetonitrile or other solvents.

Acknowledgment. This work was supported by the National Science Foundation (Grant CHE 8418611).

Registry No. AN, 107-13-1; FN, 764-42-1; TCE, 670-54-2; TS, 103-30-0; DMES, 18869-29-9.

(28) Efrima, S.; Bixon, M. *Chem. Phys.* **1976**, *13*, 447.
(29) Dogonadze, R. R.; Kuznetsov, A. M.; Vorotyntsev, M. A. *Phys. Status Solidi B* **1972**, *54*, 125.
(30) Schmickler, W. *J. Chem. Soc., Faraday Trans. 2* **1976**, *72*, 307.
(31) Marcus, R. A. *Int. J. Chem. Kinet.* **1981**, *13*, 865.
(32) Siders, P.; Cave, R. J.; Marcus, R. A. *J. Chem. Phys.* **1984**, *81*, 5613.
(33) Jortner, J. *J. Chem. Phys.* **1976**, *64*, 4860.
(34) Winstein, S.; Robinson, G. C. *J. Am. Chem. Soc.* **1958**, *80*, 169.

Microcanonical Variational Theory of Radical Recombination by Inversion of Interpolated Partition Function, with Examples: $CH_3 + H$, $CH_3 + CH_3$

Wendell Forst

Laboratoire de Physicochimie Théorique, URA 503, Université de Bordeaux I, 33405 Talence Cedex, France
(Received: July 24, 1990)

A simple interpolation scheme involving the logarithms of partition functions for initial and final states in a bond-fission reaction is used to represent, as a function of distance along the reaction coordinate, the total partition function for the transition state. The inverse Laplace transform of this partition function yields a distance-dependent state count for the transition state that serves as input for a variational routine incorporated into a standard RRKM calculation. In this way, the number of states of so-called transitional modes, in particular, is made to connect smoothly with the proper number of states of fragment rotations. The interpolation makes use of simple Morse potential for the breaking bond and one of two similar S-type switching functions: a one-parameter Gaussian and a two-parameter hyperbolic tangent, either of which gave similar results for the title recombinations, in essential agreement with experiment. It is shown that the negative temperature coefficient of a radical recombination arises primarily from the above types of switching functions, which cause a "late" switch (i.e., at large interfragment distance) to product configuration.

1. Introduction

It is generally agreed that locating the transition state (TS, properties of which are denoted by asterisk) at the centrifugal maximum of the effective potential in simple bond-fission unimolecular reactions (reactions where the reverse radical association proceeds without an energy barrier) is not the best choice since it leads to difficulties associated with the rate constant for radical association at low temperatures.[1] To alleviate this problem, a microcanonical variational criterion is now employed,[2] defined as the local minimum in $G^*(E^*,r)$, the total number of states of TS along the reaction coordinate:

$$dG^*(E^*,r)/dr = 0 \qquad (1)$$

where r is the distance along the reaction coordinate and E^* is the internal randomizable energy of the transition state (cf. eq 26). If the solution of eq 1 for a local minimum is $r = r_{min}$, then the property of interest is $G^*(E^*,r_{min})$, understood to be evaluated at $r = r_{min}$.

(1) Hase, W. L.; Wardlaw, D. M. In *Bimolecular Collisions*; Ashfold, M. N. R., Baggott, J. E., Eds.; Royal Society of Chemistry: London, 1989; Chapter 4.
(2) Wardlaw, D. M.; Marcus, R. A. *Adv. Chem. Phys.* **1987**, *70*, 231.

0022-3654/91/2095-3612$02.50/0